Proceedings of IMECE2016
2016 ASME International Mechanical Engineering Congress & Exposition
November 11-17, 2016, Phoenix, Arizona USA

IMECE2016-65253

THE ORBITLESS DRIVE

Leo Stocco, PhD, PEng
Orbitless Drives Inc.
Department of Electrical & Computer Engineering
University of British Columbia
Vancouver, British Columbia, Canada
leos@orbitless.com, leos@ece.ubc.ca

ABSTRACT

A fixed low-ratio Epicyclic drive is developed that resembles a Planetary drive but has crank-shaft pinions and an additional carrier replacing its ring gear. It provides half the reduction ratio of a Planetary drive with similar pinions, making reduction ratios at or near *2:1* practical. It shares many properties with a Planetary drive such as torque splitting and co-axial drive shafts that spin in a common direction but with no ring gear, reverse bending, or assembly criteria. It has many optional configurations and modes, does not slip or jam, is easily back-driven, has low pitch and bearing velocities, and favorable churning properties. It is a viable option for both reduction and overdrive applications that promises low noise / vibration / harshness (NVH) levels.

NOMENCLATURE

R	reduction ratio	N	number of planets
OD	outer diameter	M	tooth module
PLV	pitch line velocity	s, p, o	number of teeth
r	radius	Q	step planet ratio
Δ	offset distance	ω	angular velocity
θ	carrier angle	τ	torque
		F	force

INTRODUCTION

Fixed ratio speed reducers may be broadly classified as either high or low ratio, corresponding to kinematic arrangements providing ratios above and below approximately 10:1. Most of these are surveyed by Jelaska [6] and variations are generated in [14]. High ratio configurations are numerous and include the Worm, Cycloid, Orbit, Nutating, Harmonic [12], stepped-planet [11, figs 19-43] and bi-coupled Planetary drives. Low ratio configurations are fewer and include the Offset and Planetary drives which may be operated in Annular, Star or Solar mode, depending on which rotatable element is fixed.

A Planetary Annular drive is theoretically bounded to a minimum reduction ratio of *2:1*, with infinitely small planets, and is practically bounded to approximately *5:2*. A Star drive provides ratios as low as *-5:3* but shaft direction is reversed. A Solar drive goes as low as *11:10* but has high inertia due to its high-speed ring gear. Stepped planets reach ratios below *2:1* but small planets and yaw torques make planet design challenging.

In this paper, the Orbitless[pat.pend.] [17] drive is proposed. It is a new Epicyclic drive that shares many advantages with a Planetary drive, and may be operated in the same three modes. Additional advantages include greater suitability to modern materials [8] and tooth geometries [7], higher efficiency [4], reduced noise, vibration and harshness [3,5],

The principle of operation is presented, followed by optional configurations, modes, and the associated reduction ratios. Planet characteristics are presented which include bearing and journal size, radial bearing load, bearing and pitch line velocity, and vibration. Friction and lubrication losses are predicted and some proof of concept and commercial prototypes are built to demonstrate its characteristics with positive results.

PRINCIPLE OF OPERATION

A free-body diagram of a Planetary planet is shown in Fig. 1. F_p is the force applied by the sun and ring gear on the pitch circle and F_c is the force applied by the carrier which drives the load. At steady-state (constant speed) forces and torques sum to zero.

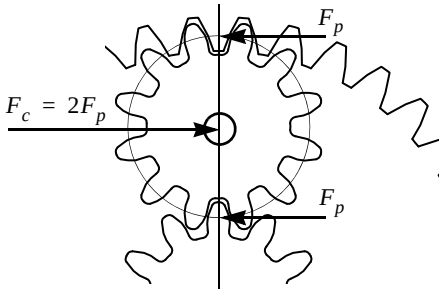

Fig. 1: Planet free-body-diagram

The role of the ring gear (Fig. 2a) is to apply the reaction force F_p that prevents the planets from spinning freely. Eliminating the ring gear (Fig. 2b) adds a degree of freedom to the drive which is removed in Fig. 2c by a second, eccentric carrier that applies a reaction force to the body of each planet. That second carrier has the same physical dimensions as the first carrier so the distance between planet axes is equal to the distance between the central axes of carriers *#1* and *#2*.

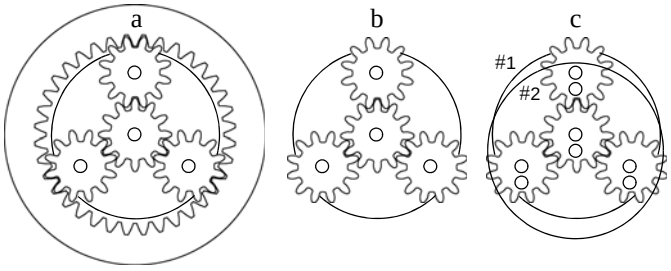

Fig. 2: Planetary (a), ring removed (b) & Orbitless (c) drives

An exploded view of an Orbitless drive is shown in Fig. 3 where carrier #1 is the drive carrier which actuates the low-speed shaft, and carrier #2 is the reaction carrier which applies a reaction force to the planets. Since the two carriers rotate in unison, either may be used as the drive or reaction carrier in practice.

The parallel, eccentric axes integrated into each planet, define a crankshaft that provides the reaction torque, normally applied to the teeth by a ring gear in a Planetary drive. The crank-shaft planets cause the carriers to rotate in unison about their individual carrier axes while the planets circulate around the sun at a fixed orientation, as shown in Fig. 4. As the sun is advanced by *90°* increments, the carriers advance in *45°* increments demonstrating a *2:1* reduction ratio.

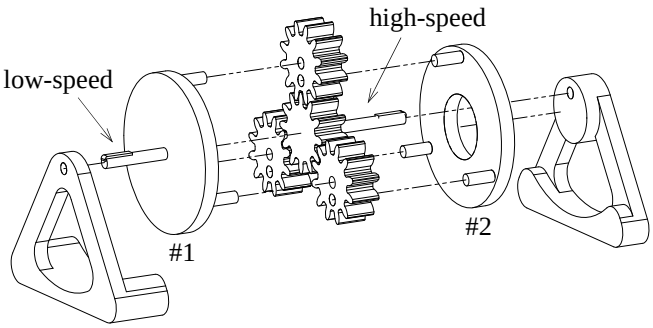

Fig. 3: Exploded Orbitless drive

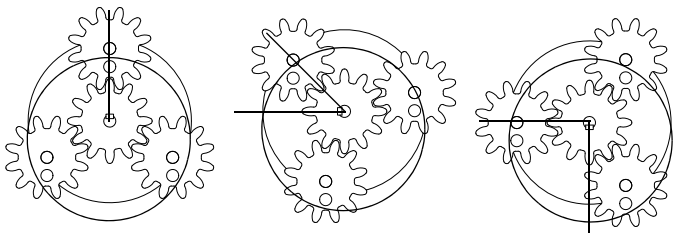

Fig. 4: 2:1 Orbitless drive at 0º, 90º & 180º (CCW)

Modes and Configurations

Just like any drive with 3 co-axial rotatable elements, an Orbitless drive may be operated in Annular, Star or Solar mode, depending on which rotatable element is fixed. The Annular mode fixes the reference member (named after the annular gear of a Planetary drive), the Star mode fixes the carrier, and the Solar mode fixes the sun.

There are also a number of possible kinematic configurations where each configuration is a unique combination of the following design options.

- The two planet axes may be positioned anywhere on the planets as long as they do not coincide.
- Either carrier may reside on either side of the planets, or may straddle the planets.
- Either carrier may be used as the drive or reaction carrier.

The “offset” configuration (Fig. 5a) combines a central reaction carrier and eccentric drive carrier. A second offset configuration (Fig. 5b) has “symmetric” planet axes that are equally spaced apart from the pinion center to maximize planet bearing size. Two “in-line” configurations (Fig. 5c,d) combine a central drive carrier with an eccentric reaction carriers to provide co-axial drive shafts. The planets in the “straddle” configuration (Fig. 5d) have an integral crankshaft that may be supported on both sides. Additional configurations are also possible.

Fig. 6 shows a variety of proof-of-concept prototypes that were constructed from ABS using a Makerbot 3D printer with brass shafts and roller bearings installed throughout. Each

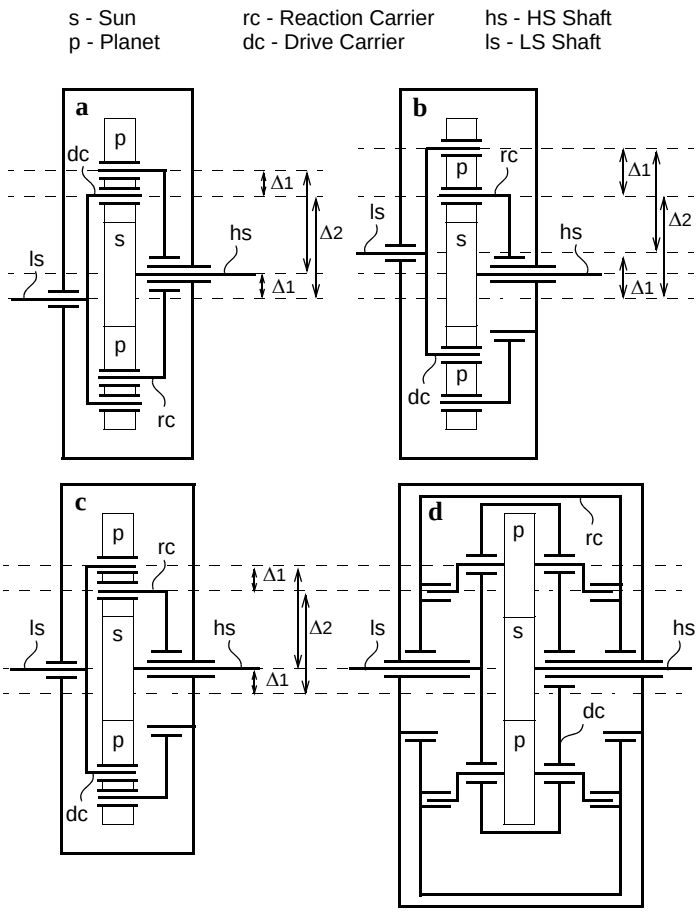

Fig. 5: Offset (a), symmetric (b), in-line (c), & straddle (d)

operates smoothly without jamming, slipping, or vibrating at speed exceeding *2,000 RPM*, and are efficiently back-driveable. A schematic appears beside each drive indicating which planet axis is connected to the drive carrier (shaded).

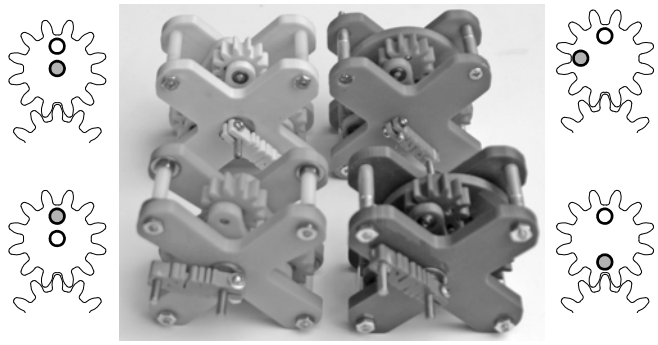

Fig. 6: Proof-of-concept prototype Orbitless drives

Reduction Ratio

The reduction ratio of an Epicyclic drive is derived by superimposing a rolling term that occurs when the carrier is fixed and the sun is rotated one turn (Star mode shown in Fig. 7) with a coupling term that occurs when the drive is rotated as a whole an arbitrary number of turns *n*. The number of coupling turns may be chosen such that any rotatable element ends up stationary to arrive at the relative number of turns for the different modes described in Table 1, where *s*, *p* and *o* are the numbers of teeth in the sun, planet and orbit (ring or annular) gears respectively. When planets are stepped, p_1 and p_2 are the numbers of teeth in the planet steps which engage the sun and ring gears respectively, and *Q* is the ratio $Q=p_2/p_1$. An Orbitless drive has no use for stepped planets since the planets only engage one gear.

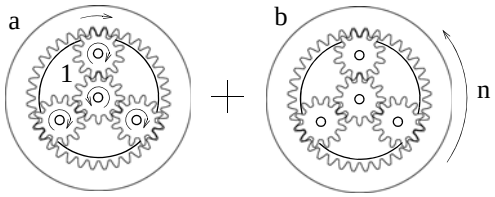

Fig. 7: Rolling (a) and coupling (b) terms

Tab. 1: Planetary rolling term and total

	Rolling Term	Planetary			
		Annular	Solar	Step	Star
Sun	o/s	1+o/s	0	1+o/Qs	o/s
Carrier	0	1	-o/s	1	0
Planet	-o/p	1-o/p	-o(p+s)/ps	1-o/p_2	-o/p
Ring	-1	0	-1-o/s	0	-1

Tab. 2: Orbitless rolling term and total

	Rolling Term	Orbitless		
		Annular	Solar	Star
Sun	p/s	1+p/s	0	p/s
Carrier	0	1	-p/s	0
Planet	-1	0	-1-p/s	-1
Case	-1	0	-1-p/s	-1

Dividing the number of input turns by the number of output turns produces the reduction ratio of a Planetary Annular (1), Solar (2), Step (3) and Star (4) drive and an Orbitless Annular (5) Solar (6) and Star (7) drive. Very small planet gears are impractical and overly large planet gears mechanically interfere so a practical constraint is applied that bounds the sun and planet geometry to differ by no more than a factor of *3* ($0.33p \le s \le 3p$). To avoid mechanical interference in a reduced-ratio Step drive, p_2 is fixed at its maximum value of $p_2=3o/7$ and *s* and p_1 are varied between $o/7$ and $3o/7$ which results in $1 \le Q \le 3$, in keeping with the factor of 3 constraint described above. This is illustrated with *3* planets ($N=3$) in Fig. 8 and results in the ranges of

practical ratios indicated in (1-7). Since gear teeth extend beyond their pitch circles in Fig. 8, some clearance is required for a reasonably large tooth module.

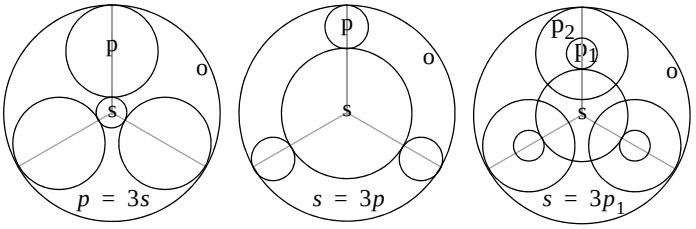

Fig. 8: Practical geometric limit of pitch circles for *N=3*

Planetary:

$$R = 1 + \frac{o}{s} = 1 + \frac{s+2p}{s} = 2\left(1 + \frac{p}{s}\right) \quad \text{Annular } 2.7 \to 8 \quad (1)$$

$$R = 1 + \frac{s}{o} = 1 + \frac{s}{s+2p} = 2\frac{s+p}{s+2p} \quad \text{Solar } 1.1 \to 1.6 \quad (2)$$

$$R = 1 + \frac{o}{Qs} = 1 + \frac{p_1(s+p_1+p_2)}{p_2 s} \quad \text{Step } 1.8 \to 8 \quad (3)$$

$$R = \frac{-o}{s} = \frac{-s-2p}{s} = -\left(1 + \frac{2p}{s}\right) \quad \text{Star } -7 \to -1.7 \quad (4)$$

Orbitless:

$$R = 1 + \frac{p}{s} \quad \text{Annular } 1.3 \to 4 \quad (5)$$

$$R = 1 + \frac{s}{p} \quad \text{Solar } 1.3 \to 4 \quad (6)$$

$$R = \frac{-p}{s} \quad \text{Star } -0.3 \to -3 \quad (7)$$

The ranges of practical ratios (1-7) are plotted in Fig. 9. The Orbitless Annular and Solar drives provide similar ratios that drop as low as *R=1.3:1*. Only a Planetary Step drive comes close at *R=1.8:1*. For negative ratios as low as *R=-1.7:1*, an Orbitless Star drive is the only option and is the only Epicyclic drive capable of both reduction and overdrive without reversing the roles of the input and output shafts.

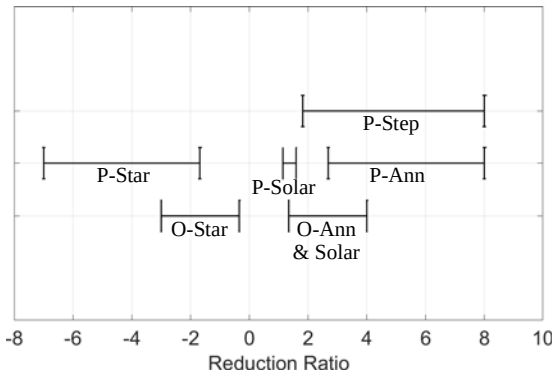

Fig. 9: Practical reduction ratios

PLANET PARAMETERS

Planet bearings are typically highly stressed and failure prone components in Epicyclic drives. Bearing life is affected by speed, radial force and yaw torque. Yaw occurs any time the vector joining two applied forces is not perpendicular to the rotation axis. For example, tooth forces on stepped planets are not co-planar so yaw results. Yaw is avoided in non-stepped planets by mounting the bearings inside the planets and the journals to the carrier(s). Then, only journal strain or other axis deviations will induce yaw. Alternatively, a carrier that straddles the planets eliminates yaw, even if the bearings are mounted in the carriers. This does not apply to stepped planets which always experience yaw regardless of bearing placement.

Bearing & Journal Radius

Planets often rely on journal bearings for their high load capacity which increases with projected area. However, load capacity may suffer if bearing diameter grows beyond bearing length due to end leakage [9, p. 191]. Nevertheless it is preferable to not to be limited by planet geometry when sizing bearings.

A cantilever carrier is more compact than a straddle carrier but the planet bearings must fit inside the planets and the carrier journals must be sufficiently large to resist strain under the rated load, otherwise planet yaw will impact efficiency and life-span. Fig. 10 shows a per-unit comparison between the relative maximum planet bearing radius of a Planetary and Orbitless drive with unity outer diameter, which is the minimum diameter that contains all pitch circles, neglecting the bulk of the case and/or ring gear. The maximum bearing radius is estimated as the planet pitch radius (of the smaller planet in the case of a stepped drive) for a Planetary drive, and half the planet pitch radius for an Orbitless drive, since each planet must contain two side by side bearings. The journal ratio is the relative Orbitless/Planetary journal radius for each of the three modes. Due to its larger planet radius, an Orbitless Solar drive is compared for all ratios *R<2:1* and an Orbitless Annular drive is compared for all ratios *R>2:1*.

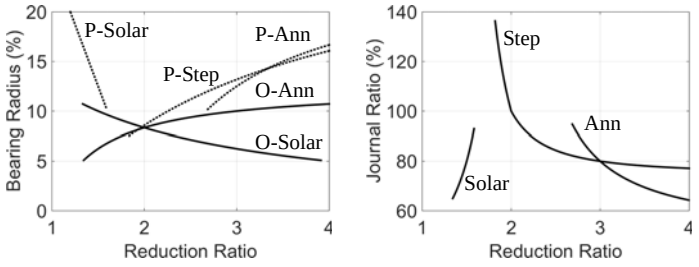

Fig. 10: Normalized bearing & journal radius

From Fig. 10, Orbitless Annular drive journals are largest for all ratios *R<2:1* and from *64%* to *95%* as large for *2:1<R<4:1*. This suggests a lower torque capacity but support provided by two parallel carrier journals may have secondary effects on torque capacity that is best determined experimentally.

Radial Bearing Load

Bearing load is dependent on many factors [17] that include geometry and carrier angle. Although the crank-shaft axes may be located anywhere on the planets, the example considered here corresponds to the in-line and straddle configurations in Fig. 5c,d. The crank-shaft axes are aligned and spaced radially from the planet center. At two carrier angles which are *180°* apart, the axes align with the sun engagement point, one of which is shown in Fig. 11. The distances r_d, r_r and r_p are the radii of the drive and reaction crank-shaft axes and the pitch line respectively. The forces $\overline{F}_d$ and $\overline{F}_r$ are the bearing forces applied by the carriers at r_d and r_r and $\overline{F}_p$ is the tooth force applied by the sun gear at r_p. At steady state, conservation of torque dictates that all forces act horizontally, perpendicular to the radial vector, and may be solved as scalars F_d, F_r. Combining the force equation (8) with the torque equation (9) produces the perpendicular force equations (10, 11) which are simplified to represent the in-line configuration used in this example.

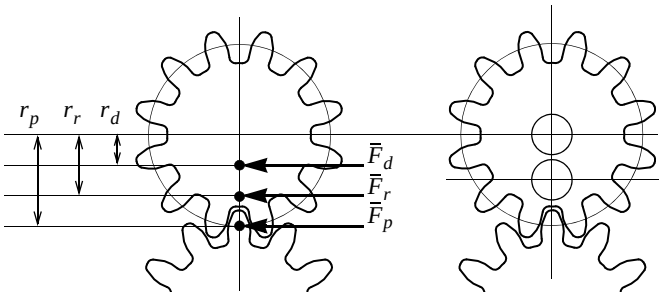

Fig. 11: Planet axis parameters

$$F_d + F_r + F_p = 0 \tag{8}$$

$$F_d r_d + F_r r_r + F_p r_p = 0 \tag{9}$$

$$\overline{F}_{d,\,0°,\,180°} = \frac{r_r - r_p}{r_d - r_r}\overline{F}_p = \left(\frac{r_p}{r_r} - 1\right)\overline{F}_p; \qquad r_d = 0 \tag{10}$$

$$\overline{F}_{r,\,0°,\,180°} = \frac{r_d - r_p}{r_r - r_d}\overline{F}_p = \frac{-r_p}{r_r}\overline{F}_p; \qquad r_d = 0 \tag{11}$$

At *θ=0°* and *θ=180°*, the perpendicular forces F_d and F_r are constant both in magnitude and direction and counteract the torque induced by pitch circle force F_p. A second, position dependent component that contributes no net torque is added to the drive carrier axis to balance the re-orienting pitch force. The net bearing force F_d at any angle θ is represented graphically by summing the static reaction force F_r to the varying pitch force F_p, where each point on the circle corresponds to a different carrier angle θ, as illustrated in Fig. 11.

A pitch circle free-body diagram of a *2:1* Orbitless drive is shown in Fig. 13. The central carrier is the drive carrier and the lower carrier is the reaction carrier. Six planet positions are shown which correspond to a drive with *N=3* planets at two

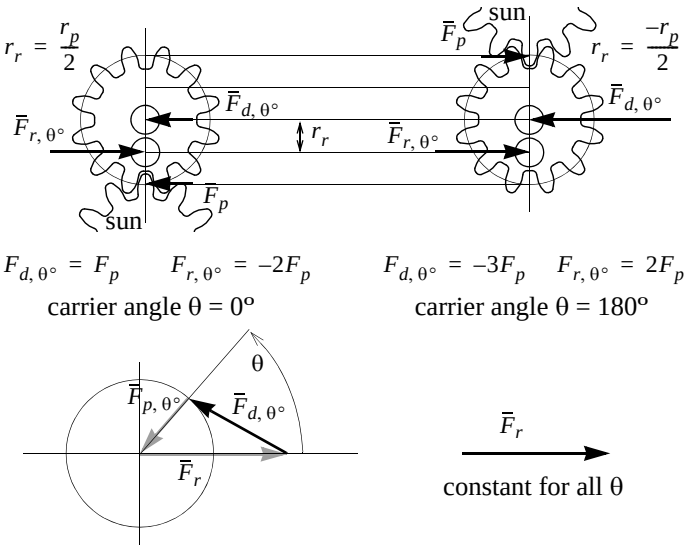

Fig. 12: Planet bearing forces

different carrier angles *θ=0°*(*a*) and *θ=180°* (*b*). The reaction carrier applies forces that are equal in magnitude and direction to each planet at all carrier angles. Due to equal circumferential spacing, this results in no net torque which is intuitive since the reaction carrier does not actuate a load.

The drive carrier has a radius of $2r_p$ and always supplies a total net torque of $6F_p r_p$. In position *a*, each journal contributes $2F_p r_p$ to the output torque while in position *b*, the bottom journal contributes $6F_p r_p$ while the forces on the other two journals are purely radial and contribute no output torque.

The reaction carrier bearing forces ($2F_p$) are equal to Planetary bearing forces (see Fig. 1) while the drive carrier forces are position dependent with a maximum magnitude of $3F_p$, which is 50% larger than Planetary bearing forces.

A straddle carrier (Fig. 5d) eliminates the $r_r<r_p$ constraint so it is practical for $r_r=r_p$, as illustrated in Fig. 14. The associated reaction forces become half as large (F_p) and drive carrier forces have a maximum magnitude of only $2F_p$, due to the longer crank-arm (r_d-r_r). This may justify a smaller journal radius one side of a straddle reaction carrier to be neglected.

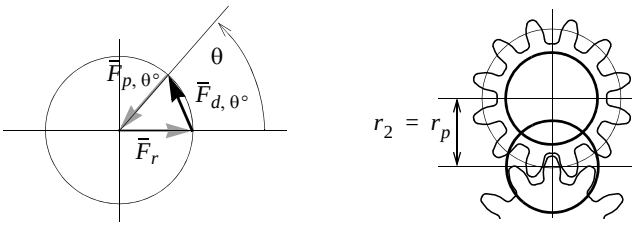

Fig. 14: Planet bearing forces with straddle carrier

From the geometry in Fig. 12, the force vectors $\overline{F}_d$ and $\overline{F}_r$ are shown as a function of carrier angle and shaft position in (12, 13),

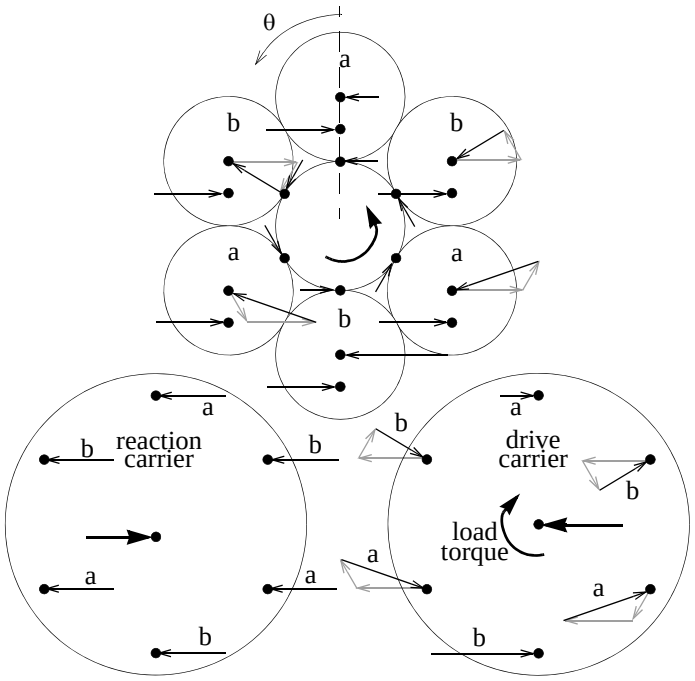

Fig. 13: Planet & carrier free-body-diagrams

their magnitudes F_d and F_r are shown in (14, 15), and plotted as a function of carrier angle in Fig. 15.

$$\bar{F}_{d,\theta} = \left[\frac{r_p}{r_2} + \cos\theta \;\; \sin\theta\right] F_p \tag{12}$$

$$\bar{F}_{r,\theta} = \left[\frac{r_p}{r_2} \;\; 0\right] F_p \tag{13}$$

$$F_{d,\theta} = \sqrt{\left(\frac{r_p}{r_2}\right)^2 + 2\frac{r_p}{r_2}\cos\theta + 1}\;\; F_p \tag{14}$$

$$F_{r,\theta} = \frac{r_p}{r_2} F_p \tag{15}$$

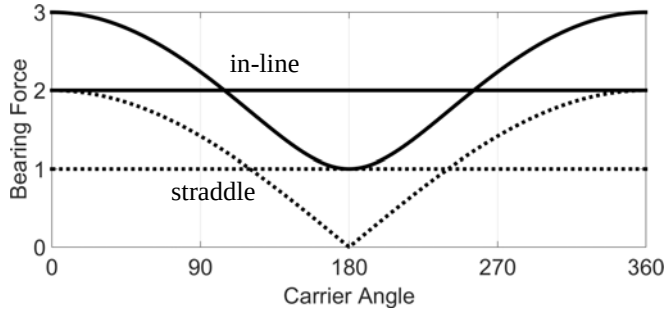

Fig. 15: Axial bearing force of in-line configurations

Bearing Speed

The load capacity of journal bearings increases with projected area and surface speed but the coefficient of friction also increases when operating in the full film regime [9, p. 187]. Beyond a critical speed, oil whip or turbulence [13] may occur. All things considered, reduced bearing speed is a desired characteristic in high-speed drives.

Epicyclic drive planets rotate on a carrier so planet bearing speed is the difference between planet speed and carrier speed, which is taken from Table 1 and rearranged as a function of reduction ratio R for a Planetary Annular (16), Solar (17), Step (18) and Star (19) drive and an Orbitless Annular (20) Solar (21) and Star (22) drive.

Planetary:

$$\frac{\omega_p - \omega_c}{\omega_s}\omega_s = \frac{(1 - o/p) - 1}{1 + o/s}\omega_s = \frac{2(1-R)}{R(R-2)}\omega_s \quad \text{Annular} \tag{16}$$

$$\frac{\omega_p - \omega_c}{\omega_o}\omega_o = \frac{-o/s + o(p+s)/ps}{-1 - o/s}\omega_o = \frac{2(1-R)}{R(R-2)}\omega_o \quad \text{Solar} \tag{17}$$

$$\frac{\omega_p - \omega_c}{\omega_s}\omega_s = \frac{(1 - o/p_2) - 1}{1 + o/Qs}\omega_s = \frac{-7}{3R}\omega_s \quad \text{Step} \tag{18}$$

$$\frac{\omega_p - \omega_c}{\omega_s}\omega_s = \frac{-s}{p}\omega_s = \frac{-2}{R+1}\omega_s \quad \text{Star} \tag{19}$$

Orbitless:

$$\frac{\omega_p - \omega_c}{\omega_s}\omega_s = \frac{-1}{1 + p/s}\omega_s = \frac{-1}{R}\omega_s \quad \text{Annular} \tag{20}$$

$$\frac{\omega_p - \omega_c}{\omega_o}\omega_o = \frac{-1 - p/s + p/s}{-1 - p/s}\omega_o = \frac{1}{R}\omega_o \quad \text{Solar} \tag{21}$$

$$\frac{\omega_p - \omega_c}{\omega_s}\omega_s = \frac{-1}{p/s}\omega_s = \frac{1}{1-R}\omega_s \quad \text{Star} \tag{22}$$

Fig. 16 shows a per-unit comparison between the bearing speed of a Planetary and an Orbitless drive with unity input speed. The input is the ring in Solar mode and the sun in all others. The speed ratio is the relative Orbitless/Planetary planet bearing speed for each mode with the Planetary Step mode compared against the Orbitless Annular mode since no Orbitless Step mode exists.

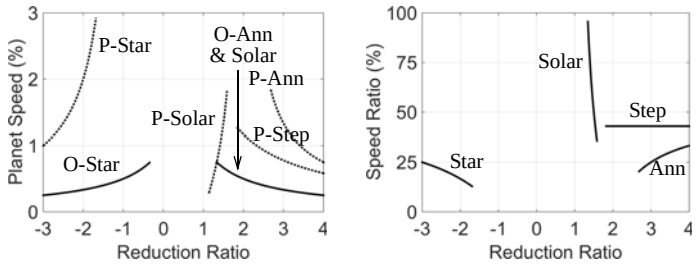

Fig. 16: Normalized planet bearing speed

From Fig. 16, Orbitless bearings spin at less than *1/4* the rate of Planetary bearings in Star mode and less than *1/2* the rate in Step or Annular mode. In Solar mode, the rate reduction is less dramatic. Recall that Orbitless planets do not rotate. They spin at the same rate as the low-speed shaft which accounts for the lower bearing rates.

Pitch Line Velocity

For an Offset or Epicyclic Star drive, pitch line velocity *PLV* is the product of input speed ω_{hs} and sun radius r_s (23). The sun radius may be written as a function of reduction ratio by applying the unity outer diameter constraint to each drive (24, 25, 26).

$$PLV = r_s \omega_{hs} \tag{23}$$

Offset: $$PLV = \frac{1}{2(1-R)}\omega_{hs} \tag{24}$$

Planetary Star: $$PLV = \frac{-1}{2R}\omega_{hs} \tag{25}$$

Orbitless Star: $$PLV = \frac{1}{2(1-2R)}\omega_{hs} \tag{26}$$

For other Epicyclic drive modes which do include a coupling component, it is shown in [1, p.298] that *PLV* is as shown in (27). This holds for both Planetary and Orbitless drives where the input gear is the sun in Annular and Step drives, the orbit ring in Planetary Solar drives, and the case which rotates in unison with the planets in Orbitless Solar drives. The input gear radius may be written as a function of reduction ratio (28, 30, 32, 34, 36) by applying the unity outer diameter constraint to each drive. It is substituted into (27) to arrive at *PLV* (29, 31, 33, 35, 37).

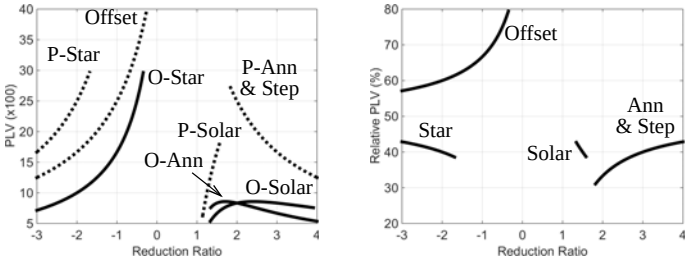

Fig. 17: Normalized pitch line velocity

From Fig. 17, an Orbitless *PLV* is well below *1/2* the *PLV* of a comparable Planetary drive in all modes. Compared to an Offset drive, an Orbitless *PLV* is between *60%* and *80%* as large. Recall that the Orbitless Solar mode can accommodate larger planet bearings than the Annular mode for all ratios R<2:1. This and its lower *PLV* make it the preferred design for lower ratios.

Vibration

The greatest source of vibration in a Planetary drive is the planets. Planet instability, inertial imbalance, tooth cogging and non-uniform wear all contribute. Planet instability is caused by redundant radial constraints imposed by the sun gear, ring gear and carrier bearing. It is addressed in practice by loosening carrier tolerances to allow self-alignment between the sun and ring [2]. While an Orbitless gear lacks a ring gear, redundant planet constraints are still imposed by the sun and two carriers. However, ring cogging is more likely to excite natural frequencies since it occurs many times per output cycle, as opposed to carrier vibrations which occur once per output cycle.

$$PLV = (\omega_{hs} - \omega_{ls}) r_{input} = r_{input}\omega_{hs}\left(1 - \frac{1}{R}\right) \tag{27}$$

Planetary:

$$r_s = \frac{1}{2(R-1)} \tag{28}$$

$$PLV = \frac{1}{2R}\omega_{hs} \tag{29}$$

Annular

$$r_s = \frac{1}{2Q(R-1)} \tag{30}$$

$$PLV = \frac{1}{2R}\omega_{hs} \tag{31}$$

Step

$$r_o = \frac{1}{2} \tag{32}$$

$$PLV = \frac{R-1}{2R}\omega_{hs} \tag{33}$$

Solar

Orbitless:

$$r_s = \frac{1}{2(R-1)} \quad \text{Annular} \tag{34}$$

$$PLV = \frac{R-1}{2R(2R-1)}\omega_{hs} = \left(\frac{1}{2R} - \frac{1}{2(2R-1)}\right)\omega_{hs} \tag{35}$$

$$r_p = \frac{1}{2(R+1)} \quad \text{Solar} \tag{36}$$

$$PLV = \frac{R-1}{2R(R+1)}\omega_{hs} = \left(\frac{1}{2R} - \frac{1}{R(R+1)}\right)\omega_{hs} \tag{37}$$

Inertial imbalance is mainly avoided by kinematic symmetry. In a Planetary drive, planets are equally spaced as long as the assemble-ability criteria (38) [9, p. 312] is satisfied. An Orbitless drive has no such assemble-ability criteria. Its planets may always be equally spaced. At worst, non-uniform crank-shaft phase angles are necessary if the uniformity criteria (39) is not satisfied.

$$\frac{s+o}{N} = \text{Integer} \tag{38}$$

$$\frac{s+p}{N} = \text{Integer} \tag{39}$$

For example, an Orbitless drive with *s=12* and *p=13* does not satisfy (39) but rotating adjacent crank-shaft angles by *120°* allows the planets to be equally spaced, as illustrated in Fig. 18.

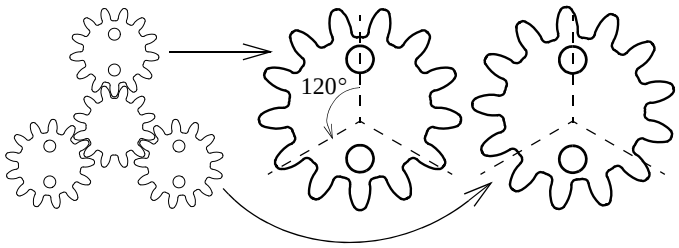

Fig. 18: Non-uniform crank-shaft phase angle

Cogging vibration is most commonly addressed by using helical gears and/or designing sequential meshing into the drive. Sequential meshing is a phase shift between tooth engagements that occur in the individual parallel transmission paths (i.e. planets). It does not eliminate cogging but spaces it out so that multiple engagements do not occur simultaneously. Amplitudes are lower, cancellations takes place, and smoother operation results. Sequential meshing is achieved by satisfying criteria (40).

$$\frac{s}{N} \neq \text{Integer} \tag{40}$$

Finally, non-uniform break-in of gear teeth may cause beats to develop over time. Hunting teeth homogenize the break-in process by ensuring that each gear tooth sequentially engages all interdental cavities on its mate. Teeth hunt when the numbers of teeth on two mated gears do not share any prime factors.

A design challenge with Planetary gears is to simultaneously satisfy the criteria for kinematic uniformity (38), sequential meshing (40) and hunting teeth, while arriving at a desired reduction ratio. It is particularly difficult to simultaneously satisfy all meshing criteria for both the sun/planet and planet/ring engagements.

Since an Orbitless drive lacks a ring gear, satisfying these criteria is much more straight forward. Take, for example, a desired ratio *R=5:2*, with 3 planets (*N=3)*, and a minimum pinion specification of *18* teeth. The sun is the smallest pinion and must not be divisible by *N=3* (40) so *19*, *20*, *22* and *23* teeth are all candidates. A planet with $p \approx 1.5s$ is rounded both up and down to satisfy (39). The candidate designs and associated prime factors and reduction ratios are shown in Table 3.

Tab. 3: Optimized 5:2 Orbitless drive parameters

Sun (s)	Planet (p)	Sun PF	Planet PF	R
19	29	19	29	2.53:1
20	31	2,5	31	2.55:1
22	32	**2**,11	**2**	2.45:1
23	34	23	2,17	2.48:1

All designs contain uniform planets and sequential meshing. The *22/32* combination shares a common prime factor (*PF=2*) but all others provide optimal hunting. With very little effort, *3* viable designs are produced which each deviate by less than *2%* from the target ratio.

EFFICIENCY

Energy losses in a gear drive include sliding and rolling losses in the gear teeth and bearings, and shearing, windage and pumping losses in the lubrication system. Friction losses are affected by a number of design factors such as module, tooth modifications, materials, bearing choice, tolerances, and many others. High precision aviation and wind power drives boast efficiencies upward of *99%* while self-locking varieties are less than *50%* efficient. A high dependence on detail design makes it difficult to analytically estimate efficiency. It is more reliable to measure it experimentally.

Nevertheless, one may qualitatively expect an Orbitless drive to have an efficiency advantage over a comparable Planetary drive, for the following reasons:

- Half as many gear engagements (3 in a 3-planet Orbitless drive as opposed to 6 in a Planetary drive). The additional planet bearings that replace the orbit ring develop less friction than gears do, in general.
- Less than half the pitch velocity. Dynamic friction increases linearly with speed so reduced friction between the sun and planets is expected.
- Less than half the bearing speed. This depends on bearing choice since journal bearing efficiency often increases with speed as long as critical speeds are not exceeded.

Lubricant Churning

Gear drive lubricants may either be forced or splashed [1]. In a forced system, lubricant is pumped through jets onto critical components, with most energy losses occurring in the pumping and hydraulics. In a splash system, partially submerged components splash or drip onto adjacent components and generate mist at high speeds, that envelops the drive. There is no hydraulic system but significant energy may be lost to churning and windage.

Since churning and windage are complex, nonlinear effects that are difficult to quantify, they are observed experimentally. For the fairest possible comparison, a Planetary and Orbitless drive are designed to have a volume, reduction ratio, gear tooth module, face width, and minimum pinion radius which are as uniform as possible. A set of gear specifications resulting in a uniform outer diameter with *R=2.8:1*, and which satisfy the assembly and uniformity criteria (38, 39), are shown in Table 4 where “o” corresponds to the *OD* of the Orbitless drive.

Prototypes are constructed with *M=3mm*, from *5mm* aluminum plate, using a waterjet cutter. All joints are self-

Tab. 4: Equivalent gear designs

	s	p	o	R
Planetary	25	11	47	2.88:1
Orbitless	10	18	(46)	2.8:1

lubricated brass journal bearings and the low-speed shaft is neglected to avoid oil leakage from the case. Although the gears are very low quality, gear quality has little effect on churning and windage. They are much more dependant on kinematics. Although circular carriers would reduce churning, triangular carriers improve visibility and are used in both drives. A transparent cover is attached and each drive is filled with equal quantities of *SAE5W40* motor oil from the same jug so that the gears are just barely submerged when laying flat.

The drives are shown at rest, revolving at *750* RPM, and again at rest after *10* seconds at *750* RPM in Fig. 19. Note that a Planetary drive defines three chambers that are surrounded by gear teeth whereas an Orbitless drive defines a single chamber with a continuous, smooth interior. The toothed chambers of the Planetary drive whip the lubricant into a light, bubbly froth while the smooth case and non-rotating planets of the Orbitless drive, stir the oil which retains a dark, liquid state at all times.

Fig. 19: Planetary (a) & Orbitless (b) drives at rest, at 750 RPM, & after 10 seconds at 750 RPM.

A motor drawing the same current was used to actuate each drive with no external load. The Planetary drive rotated at *1900 RPM* while the Orbitless drive rotated *13%* faster, at *2150 RPM*. This experiment exaggerates windage effects, so the numbers should not be interpreted as an expected efficiency gain, but rather to demonstrate that windage is in fact reduced.

Gear Members

All gearing elements in an Orbitless drive are co-planar so spur, helical, herring-bone, friction, and magnetic pinions may all be used. In addition, since Orbitless planets are only engaged by the sun, they do not experience reverse bending which reduces fatigue strength by up *30%* [1, p.102] and supports asymmetric tooth design. If stress is sufficiently reduced, plastic or other materials may be used which are light weight and inexpensive to manufacture by molding.

Its all-pinion design also supports chains or belts (Fig. 20a), and zero-backlash capstan cable drives (Fig. 20b), none of which can be used to couple internal members. In the cable drive shown in Fig. 20b, the motor is fixed to the case link and drives the sun. The planet is the reference and both the sun and case link circulate around the planet as the sun is actuated. The sun and motor counter-balance the applied load for gravity compensation.

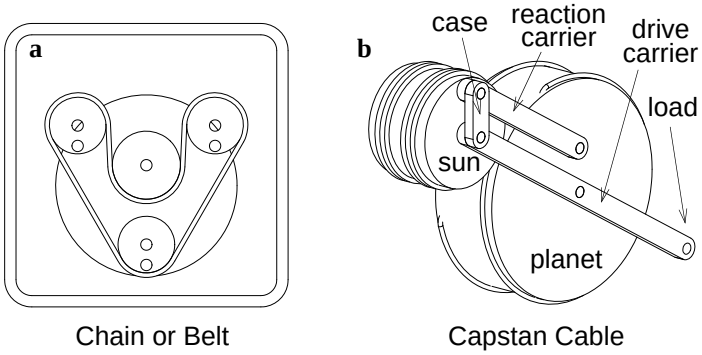

Fig. 20: Coupled Orbitless drives

In a conventional capstan drive, the reaction carrier and case links are absent. The motor is fixed to the bottom carrier link and drives the sun. The Orbitless capstan drive has a coupling component resulting in $R=1+p/s$ as opposed to $R=p/s$ for a conventional capstan drive.

COMMERCIAL PROTOTYPE

A prototype Orbitless drive (Fig. 21) was developed in collaboration with a leading manufacturer of miniature drive systems. It uses the symmetric configuration (Fig. 5b) with a *2:1* reduction ratio. All internal components were adapted from a Planetary drive rated for *5,000* RPM. The goal was to develop a *10,000 RPM 2:1* Orbitless primary stage that could be added to a *5,000 RPM* multi-stage Planetary drive, to double its speed rating and more fully exploit the abilities of brushless DC motors which can operate in excess of *20,000 RPM*. Increasing input speed, increases input power and allows a more compact motor/gear combination to satisfy a given torque/speed output requirement.

A transparent case was used to optimize the lubricant volume resulting in a pulsing ring of grease bridging the gap between the case and planets and coating the planet teeth. Initial tests up to *22,000 RPM* under light loads [10] confirmed its low noise, vibration and harshness (NVH) levels but no further data is yet available.

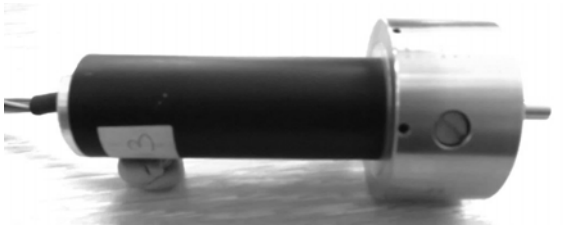

Fig. 21: Commercial prototype Orbitless drive

CONCLUSIONS

A new low-ratio Epicyclic drive is proposed and shown to possess various benefits over Planetary and Offset drives. With so few low-ratio alternatives available, there is strong potential for this new power transmission technology to provide a benefit in a number of applications. Its characteristics are as follows.

- No ring gear which is often expensive to produce.
- Optional configurations that include offset, symmetric, in-line, and straddle arrangements.
- May be operated in Annular, Solar or Star mode.
- 1/2 the reduction ratio of a Planetary Annular drive.
- Capable of almost any ratio provided by an Offset drive.
- Similar planet bearing loads as a Planetary drive.
- 50% lower bearing speed and pitch line velocity than a Planetary drive (in most modes).
- No assemble-ability criteria and easier to satisfy sequential meshing and hunting tooth criteria than a Planetary drive.
- Less friction and churning losses than a Planetary drive.
- No reverse-bending.
- Supports gears, belts, chains, and cable drives.
- Low NVH levels.

Future Work

Additional testing is to be conducted on the commercial prototype (Fig. 21), to determine quantifiable properties such as speed rating, load capacity and life-span. A high ratio Orbitless drive has also been developed that includes an intermediate coupling between the sun and planets which is the subject of another paper in these proceedings.

ACKNOWLEDGMENTS

The Research & Development group at FAULHABER MINIMOTOR SA. is gratefully acknowledged for their cooperation and support in developing and evaluating a commercial prototype.

REFERENCES

[1] N.E. Anderson, S.H. Loewenthal, J.D. Black, 1986, “An Analytical Method to Predict Efficiency of Aircraft Gearboxes”, *Trans. of the ASME Journal of Mechanisms, Transmissions, and Automation in Design*, Vol. 108, pp. 424-432.

[2] G. J. Cheon, D.H. Lee, H.T. Ryu, *A Study on the Dynamic Characteristics of an Epicyclic Gear Train with Journal Bearing*, Transmission and Driveline Symposium 1999, SAE Int.

[3] C.G. Cooley, R.G. Parker, 2014, A Review of Planetary and Epicyclic Gear Dynamics and Vibrations Research, Applied Mechanics Reviews, July 2014, Vol. 66.

[4] K. Davies, C. Chen, B.K. Chen, 2012, Complete Efficiency Analysis of Epicyclic Gear Train with Two Degrees of Freedom, Journal of Mechanical Design, Vol. 134, July 2012.

[5] T. Ericson, R. Parker, 2009, *Design and Conduct of Precision Planetary Gear Vibration Experiments*, SAE Technical Paper 2009-01-2071.

[6] D. Jelaska, 2012, *Gears and Gear Drives*, Wiley.

[7] A. Kapelevich, 2016, *Direct Gear Design for Asymmetric Tooth Gears*, Theory and Practice of Gearing and Transmissions, Mechanisms and Machine Science 34, pp. 117-143.

[8] R.E. Kleiss, A.L. Kapelevich, N.J. Kleiss Jr., 2001, *New Opportunities with Molded Gears*, AGMA Fall Technical Meeting, ISBN: 1-55589-788-6.

[9] P. Lynwander, 1983, *Gear Drive Systems*, Marcel Dekkar Inc.

[10] FAULHABER MINIMOTOR SA., 2015, *Internal Report*.

[11] H.W. Muller, 1982, *Epicyclic Drive Trains*, Wayne State Univ. Press.

[12] C.W. Musser, 1959, *Strain Wave Gearing*, US Patent #2,906,143.

[13] E.I. Radzimovsky, 1959, *Lubrication of Bearings*, The Ronald Press Company.

[14] Y.V.D. Rao, A.C. Rao, 2008, *Generation of Epicyclic Gear Trains of One Degree of Freedom*, Journal of Mechanical Design, Vol. 130, May 2008.

[15] A. Singh, 2007, *Influence of Planetary Needle Bearings on the Performance of Single and Double Pinion Planetary Systems*, Journal of Mechanical Design, Vol. 129, January 2007.

[16] G. W. Stachowiak, A.W. Atchelor, *Engineering Tribology*, 2nd ed., Butterworth Heinemann.

[17] L. J. Stocco, 2014, *Orbitless Gearbox*, Patent Cooperation Treaty, PCT/CA2015/050423.